Amitava Chatterjee
Patrick Siarry *Editors*

Computational Intelligence in Image Processing

Springer

Computational Intelligence in Image Processing

Amitava Chatterjee · Patrick Siarry
Editors

Computational Intelligence in Image Processing

Springer

Editors
Amitava Chatterjee
Electrical Engineering Department
Jadavpur University
Kolkata
West Bengal
India

Patrick Siarry
Laboratory LiSSi
University of Paris-Est Créteil
Créteil
France

ISBN 978-3-642-30620-4 ISBN 978-3-642-30621-1 (eBook)
DOI 10.1007/978-3-642-30621-1
Springer Heidelberg New York Dordrecht London

Library of Congress Control Number: 2012942025
ACM Code: I.4, I.2, J.2

Printed on acid-free paper

Springer is part of Springer Science+Business Media (www.springer.com)

Preface

Computational intelligence-based techniques have firmly established themselves as viable, alternate, mathematical tools for more than a decade now. These techniques have been extensively employed in many systems and application domains, e.g., signal processing, automatic control, industrial and consumer electronics, robotics, finance, manufacturing systems, electric power systems, power electronics and drives, etc. Image processing is also an extremely potent area which has attracted the attention of many researchers interested in the development of new computational intelligence-based techniques and their suitable applications, in both research problems and in real-world problems. Initially, most of the attention and, hence, research efforts, were focused on developing conventional fuzzy systems, neural networks, and genetic algorithm-based solutions. But, as time elapsed, more sophisticated and complicated variations of these systems and newer branches of stochastic optimization algorithms have been proposed for providing solutions for a wide variety of image processing algorithms. As image processing essentially deals with multidimensional nonlinear mathematical problems, these computational intelligence-based techniques lend themselves perfectly to provide a solution platform for these problems. The interest in this area among researchers and developers is increasing day by day and this is visible in the form of huge volumes of research works that get published in leading international journals and in international conference proceedings.

When the idea of this book was first conceived, the goal was to mainly expose the readers to the cutting-edge research and applications that are going on across the domain of image processing where contemporary computational intelligence techniques can be and have been successfully employed. The result of the spirit behind this original idea and its fruitful implementation in terms of contributions from leading researchers across the globe, in varied related fields, is in front of you: a book containing 15 such chapters. A wide cross-section of image processing problems is covered within the purview of this book. They include problems in the domains of image enhancement, image segmentation, image analysis, image compression, image retrieval, image classification and clustering, image registration, etc.

The book focuses on the solution of these problems using state-of-the-art fuzzy systems, neuro-fuzzy systems, fractals, and stochastic optimization techniques. Among fuzzy systems and neuro-fuzzy systems, several chapters demonstrate how type-2 neuro-fuzzy systems, fuzzy transforms, fuzzy vector quantization, the concept of fuzzy entropy, etc., can be suitably utilized for solving these problems. Several chapters are also dedicated to the solution of image processing problems using contemporary stochastic optimization techniques. These include several modern bio- and nature-inspired global optimization algorithms like bacterial foraging optimization, biogeography-based optimization, genetic programming (GP), along with other popular stochastic optimization strategies, namely, multi-objective particle swarm optimization techniques and differential evolution algorithms. It is our sincere belief that this book will serve as a unified destination where interested readers will get detailed descriptions of many of these modern computational intelligence techniques and they will also obtain fairly good exposure to the modern image processing problem domains where such techniques can be successfully applied.

This book has been divided into four parts. Part I concentrates on discussion of several image preprocessing algorithms. Part II broadly covers image compression algorithms. Part III demonstrates how computational intelligence-based techniques can be effectively utilized for image analysis purposes, and Part IV elucidates how pattern recognition, classification, and clustering-based techniques can be developed for the purpose of image inferencing.

Part I: Image Preprocessing Algorithms

This section of the book presents representative samples of how state-of-the-art computational intelligence-based techniques can be utilized for image preprocessing purposes, e.g., for image enhancement, image filtering, and image segmentation.

Chapter 1 by Yüksel and Baştürk shows how type-2 neuro-fuzzy systems can be utilized for developing image enhancement operators. Type-2 fuzzy systems are considered as improvements over the conventional type-1 fuzzy systems, where type-2 fuzzy systems utilize ‘fuzzy-fuzzy sets’, as opposed to the conventional ‘fuzzy sets’ utilized by the type-1 fuzzy systems. Type-2 fuzzy systems have specifically come into existence to handle data uncertainties in a better manner. This chapter shows how such general-purpose operators can be developed for a variety of image enhancement purposes. The chapter also specifically concentrates on the development of suitable new noise filters and noise detectors based on the above-mentioned methodology.

Chapter 2 by Kwok, Ha, Fang, Wang, and Chen focuses on the problem of contrast enhancement by employing a local intensity equalization strategy. The method shows how an image can be subdivided into sectors and each such sector can be independently equalized. The method employs a particle swarm optimization algorithm-based technique that determines a suitable Gaussian weighting factor-based methodology for reduction of discontinuities along sector boundaries.

Chapter 3 by Boussaïd, Chatterjee, Siarry, and Ahmed-Nacer shows how intelligent hybridization of biogeography-based optimization with differential evolution can be utilized to solve multilevel thresholding problems for image segmentation purposes, utilizing the concept of fuzzy entropy. The objective here is to incorporate diversity in the biogeography-based optimization (BBO) algorithm to solve three-level thresholding problems in a more efficient manner and to provide better uniformity for the segmented image. The utility of the proposed schemes is demonstrated for a series of benchmark images, widely utilized by the researchers within this community.

Chapter 4 by Perlin and Lopes demonstrates how GP approaches can be utilized for the development of image segmentation algorithms. This chapter shows how the image segmentation problem can be viewed as a classification problem and how GP can use a set of terminals and non-terminals to arrive at the final segmented image. The method demonstrates how suitable fitness functions can be defined and how a penalty term can be utilized to obtain a fair division of an original image into its reasonable, constituent parts, in an automated manner. The performance of the algorithm has been extensively evaluated on the basis of a set of images.

Part II: Image Compression Algorithms

Image compression techniques are becoming more and more important in recent times because the race for transmission of huge volumes of image data in real time for a wide variety of applications like Internet-based transmission, mobile communication, live transmission of television events, medical imaging, etc., is well and truly on. The main objective is to simultaneously achieve two competing requirements, i.e., to achieve very high rates of compression ratio and yet there should not be any perceptible degradation in the reconstructed image at the viewer end. This section of the book presents a collection of such modern techniques which primarily aim to solve this problem as efficiently as possible.

Chapter 5 by Tsekouras and Tsolakis describes how fuzzy clustering-based vector quantization techniques can be utilized to solve these problems. This chapter first presents a systematic overview of existing fuzzy clustering-based vector quantization techniques and then it presents a new effective fuzzy clustering-based image compression algorithm that tackles two contentious issues: (i) achieving performance independent of initialization and (ii) reducing the computational cost. The method demonstrates how hybrid clusters can be formed containing crisp and fuzzy areas.

Chapter 6 by Di Martino and Sessa demonstrates how recently proposed fuzzy transforms (F-transforms) can be utilized for layer image compression and reconstruction and then proposes a new modification. The chapter discusses how an image can be viewed as a fuzzy matrix, comprising several square submatrices, and how direct F-transforms can be suitably applied on each such image block for the compression purpose. The chapter also demonstrates how inverse F-transforms can be utilized for image reconstruction purposes at the viewer end.

Chapter 7 by Sanyal, Chatterjee, and Munshi introduces how the modified bacterial foraging optimization (BFO) algorithm can be suitably used to solve vector quantization-based image compression algorithms. This chapter shows how a nearly optimal codebook can be designed for this purpose with a high peak signal-to-noise ratio (PSNR) in the reconstructed image. The chapter also demonstrates how improvements in the chemotaxis procedure of the BFO algorithm can be useful in achieving high PSNR at the output. The utility of this algorithm is demonstrated by employing it for a variety of benchmark images.

Part III: Image Analysis Algorithms

An important research domain within the broader category of image processing is to analyze an image, captured by a suitable sensor system, for a variety of applications. Such image analysis algorithms may be solely guided by the requirement of the output of the system. In this section of the book, five chapters are included to expose the readers to five different problem domains where different aspects of image analyses are required.

Chapter 8 by Mandal, Halder, Konar, and Nagar discusses how template matching problems in a dynamic image sequence can be solved by fuzzy condition-sensitive algorithms. This chapter shows how a decision-tree-based approach can be utilized to determine the matching(s) of a given template in an entire image. A new hierarchical algorithm has been developed for this purpose and the conditions are induced with fuzzy measurements of the features. The utility of this method has been aptly demonstrated by implementing this algorithm for template matching of human eyes in facial images, under different emotional conditions.

Chapter 9 by Di Martino and Sessa presents another important application which will show how watermarking for tamper detection can be carried out for images compressed by fuzzy relation equations. This method makes use of the well-known encrypting alphabetic text Vigenère algorithm. They have used a novel, interesting method of embedding a varying binary watermark matrix in every fuzzy relation.

Chapter 10 by Bhattacharya and Das makes a detailed, systematic study on how evolutionary algorithms can be utilized for human brain registration processes, that can be useful for the purpose of brain mapping, treatment planning, image guided therapies of nervous system, etc. A new system has been developed for MR and CT image registration of human brain sections, utilizing similarity measures, for both intensity- and gradient-based images. A fuzzy c-means clustering technique has been utilized for extraction of the region of interest in each image. Any degeneracy or abnormality in human brains can be detected by utilizing this similarity metric, utilized to test the alignment between two images. These similarity metric-based objective functions are nonconvex in nature and do not lend themselves naturally for solution by conventional optimization algorithms. Hence this problem has been solved using a genetic algorithm.

Chapter 11 by Broilo and De Natale discusses how stochastic optimization algorithms can be utilized for another important image processing-based application domain, i.e., image retrieval problems. The chapter first presents an overview of the motivations behind utilizing these methods for image retrieval and several interesting methods that have so far evolved in this domain. Detailed discussions on the setting and tuning of free parameters in traditional retrieval tools as well as direct classification of images in a dataset, based on these competing stochastic algorithms, are presented. A systematic analysis on the relative merits and demerits of these methods has been presented in the context of several application examples.

Chapter 12 by Battiato, Farinella, Guarnera, Messina, and Ravì discusses an important present-day research topic in image processing, removal of red-eye artifacts in images, caused by the flash light reflected from a human retina. While the conventional preflash approaches suffer from unacceptable power consumption problems, the software-based post-acquisition correction procedures may require substantial user interaction. Many contemporary research efforts in this problem area focus on the development of suitable red eye removal techniques with as minimum visual error as possible. This chapter discusses how boosting algorithm aided classifiers can be designed for red eye recognition utilizing the concept of gray codes feature space.

Part IV: Image Inferencing Algorithms

The last section of the book presents several chapters on how modern pattern recognition-based techniques, especially those directed toward classification and clustering objectives, can be utilized for the purpose of image inferencing.

Chapter 13 by Huang, Lee, and Lin presents how fractal analysis can be useful for the purpose of pathological prostate image classification. Very recently, the use of fractal geometry for effective analysis of pathological architecture and growth of tumors has gained prominence. This chapter demonstrates how fractal dimension can be suitably utilized along with other multicategories for feature extraction from texture features, e.g., multiwavelets, Gabor filters, gray-level co-occurrence matrix, etc. These feature extraction methodologies have been coupled with several candidate classifiers, e.g., k-NN and SVM classifiers, to evaluate their relative effectiveness in classifying such prostate images. The chapter demonstrates that, in different types of classifiers developed, each time the best correct classification rates are obtained only when the feature sets include fractal dimensions. Hence the authors have justified the importance and utility of including fractal dimension-based features in prostate image classification.

Chapter 14 by Melgani and Pasolli discusses the development of multiobjective PSO algorithms for hyperspectral image clustering problems. Hyperspectral remote sensing images are quite rich in information content and they can simultaneously capture a large number of contiguous spectra from a wide range of the electromagnetic spectrum. Development of hyperspectral image classification schemes to achieve accurate data class in an unsupervised context is widely known as a challenging research problem. This chapter demonstrates how such an unsupervised clustering problem can be solved by formulating it as a multiobjective optimization problem and how a multiobjective PSO can be suitably utilized for this purpose. The authors have implemented three different statistical criteria for this purpose, i.e., the log-likelihood function, the Bhattacharyya distance, and the minimum description length. Several experimentations clearly validate the utility of the particle swarm optimizers for automated, unsupervised analysis of hyperspectral remote sensing images.

Chapter 15 by Halder, Shaw, Orea, Bhowmik, Chakraborty, and Konar details a new computational intelligence-based approach for emotion recognition from the outer lip-contour of a subject. This approach shows how the lip region of a face image can be segmented and subsequently utilized for determining the emotion. This method demonstrates how a lip-contour model can be suitably utilized for this problem and an effective hybridization of differential evolution-based optimization and support vector machine-based classification techniques have been carried out to draw the final inference. Experimental studies on a large database of human subjects have been carried out to establish the utility of the approach.

Last but not least, we would like to take this opportunity to acknowledge the contribution made by Ilhem Boussaïd, who is a faculty member in the University of Science and Technology Houari Boumediene (USTHB), Algiers, Algeria, in preparing this book in its final form. Ilhem is pursuing her own Ph.D. at the moment, performs her regular duties in her University, is the lead author of Chap. 3 of this book, and, in addition to all these, performed all LaTeX-related activities in integrating this book. We have no words left to express our gratitude to her in this matter.

Finally, the book is in its published form in front of all the readers, worldwide. We do hope that you will find this volume interesting and thought provoking. Enjoy!

Kolkata, India, August 2011 — Amitava Chatterjee
Paris, France, August 2011 — Patrick Siarry

Contents

Part I Image Preprocessing Algorithms

1 **Improved Digital Image Enhancement Filters Based on Type-2 Neuro-Fuzzy Techniques** 3
Mehmet Emin Yüksel and Alper Baştürk

2 **Locally-Equalized Image Contrast Enhancement Using PSO-Tuned Sectorized Equalization** 21
N. M. Kwok, D. Wang, Q. P. Ha, G. Fang and S. Y. Chen

3 **Hybrid BBO-DE Algorithms for Fuzzy Entropy-Based Thresholding** 37
Ilhem Boussaïd, Amitava Chatterjee, Patrick Siarry and Mohamed Ahmed-Nacer

4 **A Genetic Programming Approach for Image Segmentation** 71
Hugo Alberto Perlin and Heitor Silvério Lopes

Part II Image Compression Algorithms

5 **Fuzzy Clustering-Based Vector Quantization for Image Compression**. 93
George E. Tsekouras and Dimitrios M. Tsolakis

6 **Layers Image Compression and Reconstruction by Fuzzy Transforms** 107
Ferdinando Di Martino and Salvatore Sessa

7 Modified Bacterial Foraging Optimization Technique for Vector Quantization-Based Image Compression 131
Nandita Sanyal, Amitava Chatterjee and Sugata Munshi

Part III Image Analysis Algorithms

8 A Fuzzy Condition-Sensitive Hierarchical Algorithm for Approximate Template Matching in Dynamic Image Sequence 155
Rajshree Mandal, Anisha Halder, Amit Konar and Atulya K Nagar

9 Digital Watermarking Strings with Images Compressed by Fuzzy Relation Equations 173
Ferdinando Di Martino and Salvatore Sessa

10 Study on Human Brain Registration Process Using Mutual Information and Evolutionary Algorithms 187
Mahua Bhattacharya and Arpita Das

11 Use of Stochastic Optimization Algorithms in Image Retrieval Problems 201
Mattia Broilo and Francesco G. B. De Natale

12 A Cluster-Based Boosting Strategy for Red Eye Removal 217
Sebastiano Battiato, Giovanni Maria Farinella, Daniele Ravì, Mirko Guarnera and Giuseppe Messina

Part IV Image Inferencing Algorithms

13 Classifying Pathological Prostate Images by Fractal Analysis 253
Po-Whei Huang, Cheng-Hsiung Lee and Phen-Lan Lin

14 Multiobjective PSO for Hyperspectral Image Clustering 265
Farid Melgani and Edoardo Pasolli

15 A Computational Intelligence Approach to Emotion Recognition from the Lip-Contour of a Subject 281
Anisha Halder, Srishti Shaw, Kanika Orea, Pavel Bhowmik, Aruna Chakraborty and Amit Konar

Index 299

Part I
Image Preprocessing Algorithms

Chapter 1
Improved Digital Image Enhancement Filters Based on Type-2 Neuro-Fuzzy Techniques

Mehmet Emin Yüksel and Alper Baştürk

Abstract A general purpose image enhancement operator based on type-2 neuro-fuzzy networks is presented in this chapter. The operator can be used for a number of different image enhancement tasks depending on its training. Specifically, two different applications of the presented operator are considered here: (1) noise filter and (2) noise detector. Comparative evaluation of the performance of the presented operator is demonstrated by performing carefully designed filtering experiments. Some other areas of the possible application are also discussed.

1.1 Introduction

Digital image enhancement is one of the most active research areas in image restoration since images are inevitably corrupted by noise during image acquisition and/or transmission. As a consequence, a large number of methods have been developed and successfully employed for detecting and removing noise from digital images in the past few decades. Among these methods, the operators based on neuro-fuzzy techniques have been shown to exhibit superior performance over most of the competing operators.

In recent years, type-2 neuro-fuzzy systems and their applications have attracted a growing interest. Contrary to the scalar membership functions of conventional (type-1) fuzzy systems, the membership functions in type-2 systems are also

M. E. Yüksel (✉)
Department of Biomedical Engineering,
Erciyes University, Kayseri 38039, Turkey
e-mail: yuksel@erciyes.edu.tr

A. Baştürk
Department of Computer Engineering,
Erciyes University, Kayseri 38039, Turkey
e-mail: ab@erciyes.edu.tr

A. Chatterjee and P. Siarry (eds.), *Computational Intelligence in Image Processing*,
DOI: 10.1007/978-3-642-30621-1_1,

themselves fuzzy and it is this extra degree of fuzziness that provides the designer a more efficient handling of uncertainty, which is inevitably encountered in noisy environments. Based on this observation, image enhancement operators based on type-2 neuro-fuzzy systems may be expected to exhibit much better performance than many other existing operators, provided that appropriate network structures and processing strategies are used.

In this chapter, we begin by presenting a review of the conventional as well as state-of-the-art image restoration operators available in the literature. Following this, we propose a general-purpose image enhancement operator based on type-2 neuro-fuzzy networks. Specifically, we consider two different applications of the presented operator: noise filter and noise detector. For both applications, we perform carefully designed filtering experiments and provide comparative evaluation of the performances of the presented operator and a number of competing operators selected from the literature. We complete the chapter by giving some other areas of the possible application.

1.2 Literature Review

A large number of methods for suppressing impulse noise from digital images have been proposed in the past few decades. The majority of these methods utilize order statistics filtering, which exploits the rank order information of the pixels contained in a given filtering window. The *standard median filter* [1, 2] is probably the simplest operator to remove impulse noise and operates by changing the center pixel of the filtering window with the median of the pixels within the window. Despite its simplicity, this approach provides reasonable noise removal performance but removes thin lines and blurs image details even at low noise densities. The *weighted median filter* and the *center-weighted median filter* [3–5] attempt to avoid the inherent drawbacks of the standard median filter by giving more weight to certain pixels in the filtering window and usually demonstrate better performance in preserving image details than the standard median filter at the expense of reduced noise removal performance.

A number of methods [6–24] are based on a combination of a noise filter with an *impulse detector*, which aims to classify the center pixel of a given filtering window as corrupted or not. If the impulse detector identifies the center pixel as a corrupted pixel, its restored value is obtained by processing the pixels in the filtering window by the noise filter. Otherwise, it is passed to the output unfiltered. Although this approach considerably reduces the distortion effects of the noise filter and enhances its output, its performance inherently depends on the performance of the impulse detector. As a result, many different sorts of impulse detectors exploiting median filters [6–8], center-weighted median filters [9–12], boolean filters [13], edge-detection kernels [14], homogeneity-level information [15], statistical tests [16, 17], classifier-based methods [18], rule-based methods [19], level-detection methods [20], pixel-counting methods [21] and soft computing methods [22–24] have been developed.

In addition to the median-based filters mentioned above, various types of mean filters are successfully utilized for impulse noise removal from digital images [25–33]. Finally, there are also a number of filters based on soft computing methodologies [34–43] as well as several other nonlinear filters [44–54] that combine the desired properties of the above mentioned filters. These filters are usually more complicated, but they generally provide much better noise suppression and detail-preservation performance.

Applications of type-2 fuzzy logic systems [55–65] in digital image processing have shown a steady increase in the last decade. Type-2 fuzzy logic-based image processing operators are usually more complicated than conventional and type-1 based operators. However, they usually yield better performance. Successful applications include gray-scale image thresholding [66], edge detection [67–70], noise-filtering [71–74], corner and edge detection in color images [75], deinterlacing of video signals [76] and image enhancement [77].

1.3 The Type-2 NF Operator

1.3.1 The Structure of the Operator

Figure 1.1a shows the general structure of the neuro-fuzzy image enhancement operator. The operator is constructed by combining a desired number of type-2 neuro-fuzzy (NF) blocks, defuzzifiers and a postprocessor. The operator processes the pixels contained in its filtering window (Fig. 1.1b) and generates an output based on type-2 fuzzy inference. Each NF block in the structure processes a different neighborhood relationship between the center pixel of the filtering window and two neighboring pixels. Possible neighborhood topologies are shown in Fig. 1.1c.

All NF blocks employed in the structure of the operator are identical to each other and function as suboperators. However, it should be observed that the values of the internal parameters of each of the NF blocks are different from those in the other NF blocks, even though all NF blocks have the same internal structure and the same number of internal parameters. This is because each NF block is trained for its particular neighborhood individually and independently of the others during training, which is discussed in detail later.

Each NF block accepts the center pixel and two of its appropriate neighboring pixels as input and produces an output, which is a *type-1 interval fuzzy set* representing the uncertainty interval (i.e., lower and upper bounds) for the restored value of the center pixel. The output fuzzy sets coming from the NF blocks are then fed to the corresponding defuzzifier blocks. The defuzzifier defuzzifies the input fuzzy set and converts it into a single scalar value. These scalar values are finally evaluated by the postprocessor and converted into a single output value, which is also the output value of the overall system.

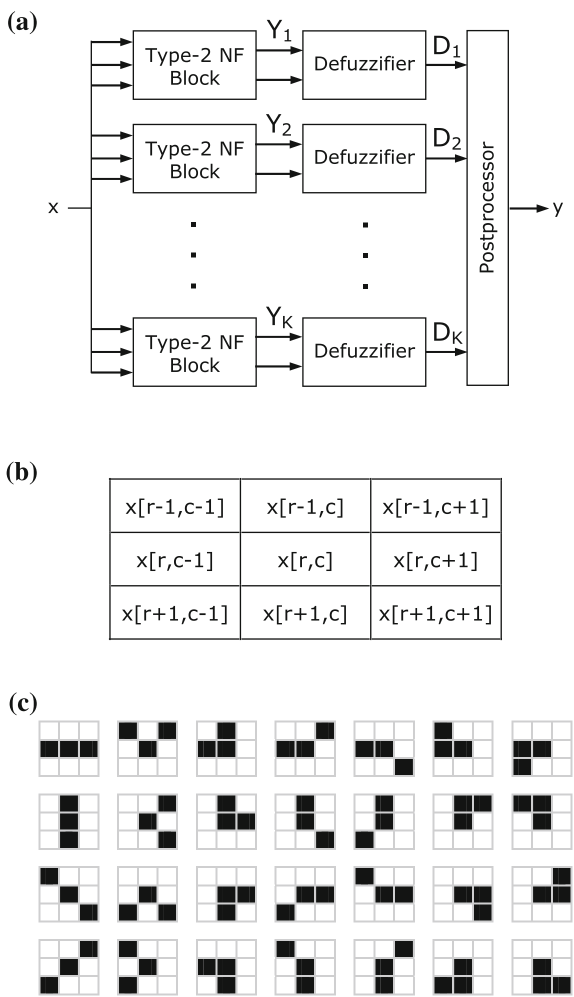

Fig. 1.1 **a** Structure of the general purpose type-2 neuro-fuzzy image enhancement operator, **b** filtering window of the operator, **c** possible pixel neighborhood topologies (Reproduced from [73] with permission from the IEEE. © 2008 IEEE.)

1.3.2 Type-2 NF Blocks

Each NF block employed in the structure of the presented image enhancement operator is a Sugeno-type first-order type-2 interval fuzzy inference system with three inputs and one output. The internal structures of the NF blocks are identical to each other. The input-output relationship of any of the NF blocks is as follows:

Let X_1^k, X_2^k, X_3^k denote the inputs of the kth NF block and Y_k denote its output. Each combination of inputs and their associated membership functions is represented by a rule in the rule-base of the kth NF block. The rule-base contains a desired number of fuzzy rules, which are as follows:

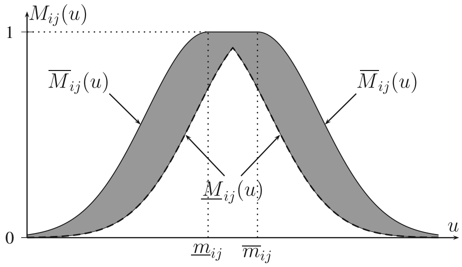

Fig. 1.2 A type-2 interval Gaussian membership function with uncertain mean. The *shaded area* is the footprint of uncertainty (FOU) (Reproduced from [73] with permission from the IEEE. © 2008 IEEE.)

1. if $(X_1^k \in M_{11}^k)$ & $(X_2^k \in M_{12}^k)$ & $(X_3^k \in M_{13}^k)$, then $R_1^k = c_{11}^k X_1^k + c_{12}^k X_2^k + c_{13}^k X_3^k + c_{14}^k$
2. if $(X_1^k \in M_{21}^k)$ & $(X_2^k \in M_{22}^k)$ & $(X_3^k \in M_{23}^k)$, then $R_2^k = c_{21}^k X_1^k + c_{22}^k X_2^k + c_{23}^k X_3^k + c_{24}^k$
3. if $(X_1^k \in M_{31}^k)$ & $(X_2^k \in M_{32}^k)$ & $(X_3^k \in M_{33}^k)$, then $R_3^k = c_{31}^k X_1^k + c_{32}^k X_2^k + c_{33}^k X_3^k + c_{34}^k$

$\vdots \qquad\qquad\qquad\qquad \vdots$

i. if $(X_1^k \in M_{i1}^k)$ & $(X_2^k \in M_{i2}^k)$ & $(X_3^k \in M_{i3}^k)$, then $R_i^k = c_{i1}^k X_1^k + c_{i2}^k X_2^k + c_{i3}^k X_3^k + c_{i4}^k$

$\vdots \qquad\qquad\qquad\qquad \vdots$

N. if $(X_1^k \in M_{N1}^k)$ & $(X_2^k \in M_{N2}^k)$ & $(X_3^k \in M_{N3}^k)$, then $R_N^k = c_{N1}^k X_1^k + c_{N2}^k X_2^k + c_{N3}^k X_3^k + c_{N4}^k$

where N is the number of fuzzy rules in the rule-base, M_{ij}^k denotes the ith membership function of the jth input and R_i^k denotes the output of the ith rule.

The antecedent membership functions are type-2 interval Gaussian membership functions with uncertain mean:

$$M_{ij}^k(u) = \exp\left[-\frac{1}{2}\left(\frac{u - m_{ij}^k}{\sigma_{ij}^k}\right)^2\right] \quad m_{ij}^k \in [\underline{m}_{ij}^k, \overline{m}_{ij}^k] \tag{1.1}$$

with $i = 1, 2, \cdots, N$; $j = 1, 2, 3$ and $k = 1, 2, \cdots, K$. Here, the parameters m_{ij}^k and σ_{ij}^k are the *mean* and the *standard deviation* of the type-2 interval Gaussian membership function M_{ij}^k, respectively, and the interval $[\underline{m}_{ij}^k, \overline{m}_{ij}^k]$ denotes the lower and the upper bounds of the uncertainty in the mean. A sample type-2 interval Gaussian membership function and its associated *footprint of uncertainty (FOU)* are illustrated in Fig. 1.2.

Since the membership functions M_{ij}^k are *interval* membership functions, the boundaries of their FOU are characterized by their *lower* and *upper* membership functions, which are defined as

$$\underline{M}_{ij}^{k}(u) = \begin{cases} \exp\left[-\frac{1}{2}\left(\frac{u-\underline{m}_{ij}^{k}}{\sigma_{ij}^{k}}\right)^2\right] & u > \frac{\underline{m}_{ij}^{k}+\overline{m}_{ij}^{k}}{2} \\ \exp\left[-\frac{1}{2}\left(\frac{u-\overline{m}_{ij}^{k}}{\sigma_{ij}^{k}}\right)^2\right] & u \leq \frac{\underline{m}_{ij}^{k}+\overline{m}_{ij}^{k}}{2} \end{cases} \tag{1.2}$$

and

$$\overline{M}_{ij}^{k}(u) = \begin{cases} \exp\left[-\frac{1}{2}\left(\frac{u-\underline{m}_{ij}^{k}}{\sigma_{ij}^{k}}\right)^2\right] & u < \underline{m}_{ij}^{k} \\ 1 & \underline{m}_{ij}^{k} \leq u \leq \overline{m}_{ij}^{k} \\ \exp\left[-\frac{1}{2}\left(\frac{u-\overline{m}_{ij}^{k}}{\sigma_{ij}^{k}}\right)^2\right] & u > \overline{m}_{ij}^{k} \end{cases} \tag{1.3}$$

where $\underline{M}_{ij}^{k}$ and $\overline{M}_{ij}^{k}$ are the lower and the upper membership functions of the type-2 interval membership function M_{ij}^{k}, respectively.

The output of the kth NF block is the weighted average of the individual rule outputs:

$$Y_k = \frac{\sum_{i=1}^{N} w_i^k R_i^k}{\sum_{i=1}^{N} w_i^k} \tag{1.4}$$

The weighting factor, w_i^k, of the ith rule is calculated by evaluating the membership expressions in the antecedent of the rule. This is accomplished by first converting the input values to fuzzy membership values by utilizing the antecedent membership functions M_{ij}^{k} and then applying the *and* operator to these membership values. The *and* operator corresponds to the multiplication of the antecedent membership values:

$$w_i^k = M_{i1}^{k}(X_1^k)\,.\,M_{i2}^{k}(X_2^k)\,.\,M_{i3}^{k}(X_3^k) \tag{1.5}$$

Since the membership functions M_{ij}^{k} in the antecedent of the ith rule are type-2 interval membership functions, the weighting factor w_i^k is a type-1 interval set, i.e., $w_i^k = [\underline{w}_i^k, \overline{w}_i^k]$, whose lower and upper boundaries are determined by using the lower and the upper membership functions defined before:

$$\begin{aligned} \underline{w}_i^k &= \underline{M}_{i1}^{k}(X_1^k)\,.\,\underline{M}_{i2}^{k}(X_2^k)\,.\,\underline{M}_{i3}^{k}(X_3^k) \\ \overline{w}_i^k &= \overline{M}_{i1}^{k}(X_1^k)\,.\,\overline{M}_{i2}^{k}(X_2^k)\,.\,\overline{M}_{i3}^{k}(X_3^k) \end{aligned} \tag{1.6}$$

where $\underline{w}_i^k$ and $\overline{w}_i^k$ $(i = 1, 2, \cdots, N)$ are the lower and upper boundaries of the interval weighting factor w_i^k of the ith rule, respectively.

After the weighting factors are obtained, the output Y_k of the kth NF filter can be found by calculating the weighted average of the individual rule outputs by using Eq. (1.4). The output Y_k is also a type-1 interval set, i.e., $Y_k = [\underline{Y}_k, \overline{Y}_k]$, since the w_i^ks in the above Eq. are type-1 interval sets and the R_i^ks are scalars. The lower and the upper boundaries of Y_k are determined by using the iterative procedure proposed by Karnik and Mendel [78].

1.3.3 The Defuzzifier

The defuzzifier block takes the type-1 interval fuzzy set obtained at the output of the corresponding NF block as input and converts it into a scalar value by performing centroid defuzzification. Since the input set is a type-1 interval fuzzy set, i.e., $Y_k = [\underline{Y}_k, \overline{Y}_k]$, its centroid is equal to the center of the interval:

$$D_k = \frac{\underline{Y}_k + \overline{Y}_k}{2} \tag{1.7}$$

1.3.4 The Postprocessor

The postprocessor generates the final output of the proposed operator. It processes the scalar values obtained at the outputs of the defuzzifiers and produces a single scalar output, which represents the output of the operator.

The postprocessor actually calculates the average value of the defuzzifier outputs and then suitably truncates this value to an 8-bit integer number. The input-output relationship of the postprocessor may be explained as follows:

Let $D_1, D_2, \cdots, D_K$ denote the outputs of the defuzzifiers in the structure of the proposed operator (Fig. 1.1a). The output of the postprocessor is calculated in two steps. In the first step, the average value of the individual type-2 NF block outputs is calculated:

$$D_{AV} = \frac{1}{K} \sum_{k=1}^{K} D_k \tag{1.8}$$

In the second step, this value is suitably truncated to an 8-bit integer value so that the luminance value obtained at the output of the postprocessor ranges between 0 and 255:

$$y = \begin{cases} 0 & \text{if } D_{AV} < 0 \\ 255 & \text{if } D_{AV} > 255 \\ \text{round}(D_{AV}) & \text{otherwise} \end{cases} \tag{1.9}$$

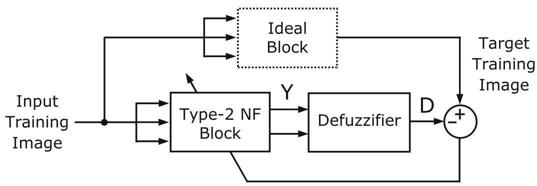

Fig. 1.3 General setup for training the type-2 NF blocks in the structure of the image enhancement operator (Adapted from [73] with permission from the IEEE. © 2008 IEEE.)

where y is the output of the postprocessor, which is also the output of the type-2 NF image enhancement operator.

1.3.5 Training the NF Blocks

The internal parameters of the proposed operator are optimized by training. Training of the proposed operator is accomplished by training the individual type-2 NF blocks in its structure. Each NF block in the structure is trained individually and independently of the others. The training setup is shown in Fig. 1.3.

The parameters of the NF block under training are iteratively adjusted in such a manner that its output converges to the output of the ideal block. The ideal block is conceptual only and does not necessarily exist in reality. It is only the output of the ideal block that is necessary for training and this is represented by a suitably chosen target training image, which varies depending on the application.

The parameters of the NF block under training are tuned by using the Levenberg Marquardt optimization algorithm [79–81] so as to minimize the learning error. Once the training of the NF blocks is completed, the internal parameters of the blocks are fixed, and the blocks are combined with the same number of defuzzifiers and a postprocessor to construct the NF operator (Fig. 1.1a).

1.3.6 Processing the Input Image

The overall procedure for processing the input image may be summarized as follows:

1. A 3×3 pixel filtering window is slid over the image one pixel at a time. The window is started from the upper-left corner of the image and moved sideways and progressively downwards in a *raster scanning* fashion.
2. For each filtering window position, the appropriate pixels of the filtering window representing the possible neighborhoods of the center pixel are fed to the corresponding NF blocks in the structure. Each NF block individually generates a type-1 interval fuzzy set as its output.

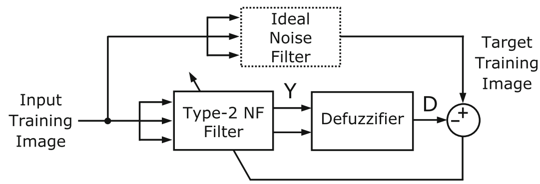

Fig. 1.4 Setup for training the type-2 NF filters in the structure of the image enhancement operator for the noise filter application (Reproduced from [73] with permission from the IEEE. © 2008 IEEE.)

3. The outputs of the NF blocks are fed to their corresponding defuzzifiers. The defuzzifiers process the input type-1 interval fuzzy sets coming from the NF blocks and output the centroid of their input sets.
4. The outputs of the defuzzifiers are fed to the postprocessor, which processes the scalar values obtained at the outputs of the defuzzifiers and produces a single scalar output. The value obtained at the output of the postprocessor is also the output value of the operator.
5. This procedure is repeated for all pixels of the noisy input image.

1.4 Applications

In this section, we demonstrate two different applications of the type-2 NF image enhancement operator presented in the previous section: noise filtering and noise detection. In both of these applications, the same general purpose type-2 NF operator shown in Fig. 1.1 are used. However, a different pair of training images is used in the training to customize the operator for each of these two applications.

1.4.1 The Type-2 NF Operator as a Noise Filter

In the first application, we demonstrate the use of the type-2 NF image enhancement operator as a noise filter. The training arrangement to customize an individual NF block in the structure of the operator as a noise filter is illustrated in Fig. 1.3. Here, the parameters of the NF block under training are iteratively tuned to minimize the difference between its output and the output of the ideal noise filter. The ideal noise filter is a conceptual filter that is capable of completely removing the noise from the image and does not necessarily exist in reality. What is necessary for training is only the output of the ideal noise filter, which is represented by the target training image.

Figure 1.4 shows the training setup for the noise filter application and Fig. 1.5 shows the images used for training. The training image shown in Fig. 1.5a is a computer-generated 40×40 pixel artificial image. Each square box in this image has a size of 4×4 pixels and the 16 pixels contained within each box have the same luminance value, which is an 8-bit integer number uniformly distributed between

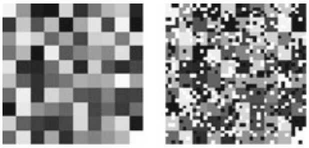

Fig. 1.5 Training images: **a** Original training image, s **b** Noisy training image (Reproduced from [73] with permission from the IEEE. © 2008 IEEE.)

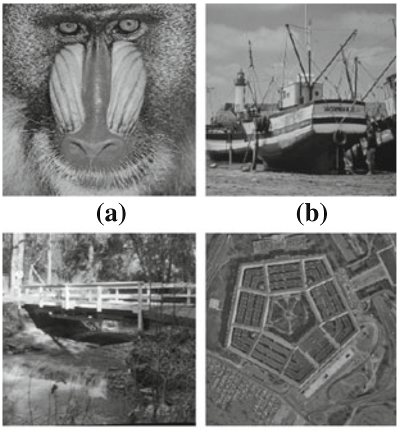

Fig. 1.6 Test images: **a** Baboon, **b** Boats, **c** Bridge, **d** Pentagon (Reproduced from [73] with permission from the IEEE. © 2008 IEEE.)

0 and 255. The image in Fig. 1.5b is obtained by corrupting the image in Fig. 1.5a by impulse noise of 30 % noise density. The images in Fig. 1.5a and b are employed as the target (desired) and the input images during training, respectively.

Several filtering experiments are performed to evaluate the filtering performance of the presented type-2 NF operator functioning as a noise filter. The experiments are especially designed to reveal the performance of the operator for different image properties and noise conditions.

Figure 1.6 shows the test images used in the experiments. Noisy experimental images are obtained by contaminating the original test images by impulse noise with an appropriate noise density depending on the experiment. For comparison, the corrupted experimental images are also restored by using a number of conventional as well as state-of-the-art impulse noise removal operators from the literature, including the standard median filter (MF) [1, 2], the switching median filter (SMF) [6], the tristate median filter (TSMF) [9], the signal-dependent rank-ordered mean filter (SDROMF) [26], the fuzzy filter (FF) [36], the progressive switching median filter (PSMF) [7], the multistate median filter (MSMF) [11], the edge-detecting median filter (EDMF) [14], the adaptive fuzzy switching filter (AFSF) [51], the alpha-trimmed mean-based filter (ATMBF) [33] and the adaptive median filter with difference-type noise detector (DNDAM) [19].

The performance of all operators is evaluated by using the mean-squared error (MSE) criterion, which is defined as

Table 1.1 Average MSE values of operators for 25, 50 and 75 % noise densities (Reproduced from [73] with permission from the IEEE. © 2008 IEEE.)

Filter	25 %	50 %	75 %	Average
MF	505	2367	8460	3777
SMF	421	2324	8454	3733
TSMF	632	3742	10996	5123
SDROMF	328	802	4067	1732
FF	265	734	3061	1353
PSMF	301	576	2640	1172
MSMF	612	3640	10317	4856
EDMF	298	1007	4955	2086
AFSF	271	547	1759	859
ATMBF	431	2333	8459	3741
DNDAM	371	800	2640	1270
Type-2 NF	145	382	980	502

$$\mathrm{MSE} = \frac{1}{RC} \sum_{r=1}^{R} \sum_{c=1}^{C} (s[r,c] - y[r,c])^2 \tag{1.10}$$

where $s[r, c]$ and $y[r, c]$ represent the luminance values of the pixels at location (r, c) of the original and the restored versions of a corrupted test image, respectively.

Table 1.1 shows the average MSE values of all operators included in the noise-filtering experiments. Here the average MSE value of a given operator for a given noise density is found by averaging the four MSE values of that operator obtained for four test images. It is seen from this Table that the proposed operator offers the best performance of all operators.

1.4.2 The Type-2 NF Operator as a Noise Detector

All image restoration filters more or less damage the uncorrupted pixels of their input image while repairing the corrupted (noisy) pixels, thus introducing undesirable blurring effects into the repaired output image. This problem can be avoided by using a special operator, called an *impulse detector*, that is capable of distinguishing the corrupted pixels of the input image from the uncorrupted ones. Hence, an impulse detector is used to guide a noise filter during its processing of the noisy input image and improve its performance. If the input pixel under concern is classified as uncorrupted, then it is passed to the output image without filtering. If it is classified as corrupted, its restored version produced by the noise filter is passed to the output image. Various different types of impulse detectors [6–24] have been shown in the

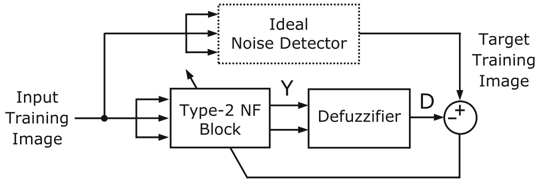

Fig. 1.7 Setup for training the type-2 NF filters in the structure of the image enhancement operator for the noise detector application. (Adapted from [73] with permission from the IEEE. © 2008 IEEE.)

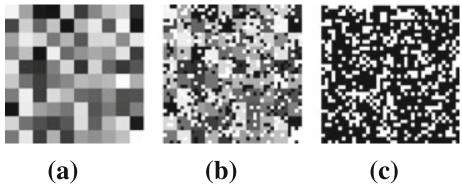

Fig. 1.8 Training images: **a** Original training image, **b** Noisy training image, **c** Noise-detection image (Reproduced and adapted from [73] with permission from the IEEE. © 2008 IEEE.)

last decade to significantly improve the performance and reduce the blurring effects of image noise removal operators.

In this section, we demonstrate the use of the presented type-2 NF operator as a noise detector. We first demonstrate how to customize the general-purpose type-2 NF image enhancement operator as a noise detector, and then we demonstrate how to use it together with a noise filter to improve the performance of that filter.

The arrangement used for training an individual type-2 NF block in the structure of the NF operator as a noise detector is illustrated in Fig. 1.7. Here, the internal parameters of the NF block under training are iteratively adjusted so that its output converges to the output of the ideal noise detector. The ideal noise detector is again a conceptual operator, and its output is represented by the noise-detection image shown in Fig. 1.8c.

Figure 1.8 shows the three training images used for the noise-detection application: the original training image, the noisy training image and the noise-detection image *from left to right*. The first two images, the original and the noisy training images, are the same as the ones used in the noise-filtering application. The third image, the noise-detection image, deserves a little explanation. It is obtained from the difference between the original training image and the noisy training image. Locations of the white pixels in this image indicate the locations of the noisy pixels. Hence, it is not difficult to see that the images in Fig. 1.8c and b are used as the target (desired) and the input images for noise detection training process, respectively.

The enhanced filtering process of a given noisy input image comprises three stages. In the first stage, the noisy input image is fed to the noise filter, which generates a repaired image at its output. In the second stage, the noisy input image is fed to the type-2 NF impulse detector, which generates a noise-detection image at its output. The noise-detection image is a black-and-white image that is similar to the target training image (Fig. 1.8c). In the third stage, the pixels of the noisy input image and the repaired output image are appropriately mixed to obtain the enhanced output image. For this purpose, those pixels of the enhanced output image that correspond

Table 1.2 MSE values for the noise-detection application

Filter	MSE without detector	MSE with detector
MF	497	195
EDMF	301	193
MMEMF	258	110

to the white pixels of the noise-detection image are copied from the repaired output image of the noise filter, while the others are copied directly from the original input image.

The validity of the method discussed above is demonstrated by using it with three different noise filters. These are the MF [1, 2], the EDMF [14] and the minimum maximum exclusive mean filter (MMEMF) [30].

Table 1.2 shows the average MSE values for the three filters for the uses "without" and "with" the detector for the baboon image corrupted by impulse noise with 25 % noise density. As can easily be seen from the Table, the detector significantly reduces the average MSE values of the filters. For a visual evaluation of the enhancement obtained by using the type-2 NF detector, the output images of the three noise filters for the uses "without" and "with" the detector for the baboon image corrupted by impulse noise with 25 % noise density are given in Fig. 1.9. For each vertical image pair in this figure, the upper image shows the direct output image of the corresponding noise filter while the lower image shows the image enhanced by using the noise filter with the type-2 NF noise detector. The undesirable blurring effects and the restoration of these distortions by means of the type-2 NF noise detector can clearly be observed by carefully examining the small details and texture in the images, such as the hair around the baboon's mouth.

1.5 Conclusions and Remarks

In this chapter, we presented an improved image enhancement operator based on type-2 NF networks. The presented operator is a general purpose operator that can be customized for a number of different tasks in image processing. We presented two specific applications here: noise filter and noise detector.

It should be pointed out, however, that other potential application areas of the general-purpose NF operator structure discussed here are not limited to the two applications presented in this chapter The presented NF operator may be used for a number of other applications in image processing provided that appropriate network topologies and training strategies are employed. In this way, it is straightforward to obtain the type-2 versions of the type-1 applications presented in [82, 83] by simply replacing the type-1 operator in the training setup by a type-2 one and appropriately choosing the training images. Other potential applications are left to the reader.

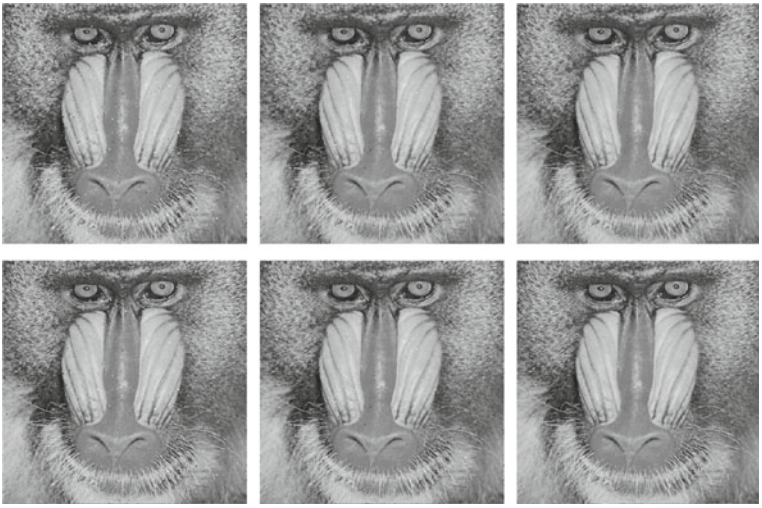

Fig. 1.9 Output images of three noise filters for the noise-detection application, comparing the noise filters with (*lower*) and without (*upper*) the type-2 NF noise detector: **a** MF, **b** EDMF, **c** MMEMF

Acknowledgments Part of the material (text, Eqs., figures, etc.) from a previously published work of the authors [73] copyrighted by the IEEE (© 2008 IEEE) has been adapted and/or reused in Sects. 1.2, 1.3 and 1.4.1 of this chapter. The authors wish to thank the IEEE for its kind permission to reuse this material.
Part of the results presented in this chapter were obtained during two research projects funded by the Erciyes University Scientific and Technological Research Center (Project code: FBT-07-12) and the Turkish Scientific and Technological Research Council (TÜBİTAK, project code: 110E051). The authors also wish to thank Erciyes University and TÜBİTAK for their kind support of this work.

References

1. Gabbouj, M., Coyle, E.J., Gallager, N.C.: An overview of median and stack filtering. Circuits Syst. Signal Process. **11**, 7–45 (1992)
2. Umbaugh, S.E.: Computer Vision and Image Processing. Prentice-Hall International Inc, Upper Saddle River (1998)
3. Yli-Harja, O., Astola, J., Neuvo, Y.: Analysis of the properties of median and weighted median filters using threshold logic and stack filter representation. IEEE Trans. on Signal Process. **39**, 395–410 (1991)
4. Ko, S.J., Lee, Y.H.: Center weighted median filters and their applications to image enhancement. IEEE Trans. Circuit Syst. **38**, 984–993 (1991)
5. Yin, L., Yang, R., Gabbouj, M.: Weighted median filters: A tutorial. IEEE Trans. Circuits Syst. **II**(43), 157–192 (1996)

6. Sun, T., Neuvo, Y.: Detail-preserving median based filters in image processing. Pattern Recognit. Lett. **15**, 341–347 (1994)
7. Wang, Z., Zhang, D.: Progressive switching median filter for the removal of impulse noise from highly corrupted images. IEEE Trans. Circuit Syst. **46**, 78–80 (1999)
8. Khryashchev, V.V., Apalkov, I.V., Priorov, A.L.: Image denoising using adaptive switching median filter. In: Proceedings of the IEEE International Conference on Image Processing (ICIP'2005), vol. 1, pp. 117–120 (2005)
9. Chen, T., Ma, K.K., Chen, L.H.: Tri-state median filter for image denoising. IEEE Trans. Image Process. **8**, 1834–1838 (1999)
10. Chen, T., Wu, H.R.: Adaptive impulse detection using center-weighted median filters. IEEE Signal Proc. Lett. **8**, 1–3 (2001)
11. Chen, T., Wu, H.R.: Space variant median filters for the restoration of impulse noise corrupted images. IEEE Trans. Circuit Syst. II, **48**, 784–789 (2001)
12. Chan, R.H., Hu, C., Nikolova, M.: An iterative procedure for removing random-valued impulse noise. IEEE Signal Proc. Lett., **11**, 921–924 (2004)
13. Aizenberg, I., Butakoff, C., Paliy, D.: Impulsive noise removal using threshold boolean filtering based on the impulse detecting functions. IEEE Signal Proc. Lett. **12**, 63–66 (2005)
14. Zhang, S., Karim, M.A.: A new impulse detector for switching median filters. IEEE Signal Proc. Lett. **9**, 360–363 (2002)
15. Pok, G., Liu, Y., Nair, A.S.: Selective removal of impulse noise based on homogeneity level information. IEEE Trans. Image Process. **12**, 85–92 (2003)
16. Beşdok, E., Yüksel, M.E.: Impulsive noise rejection from images with Jarque–Berra test based median filter. Int. J. Electron. Commun. (AEÜ) **59**, 105–110 (2005)
17. Garnett, R., Huegerich, T., Chui, C.: A universal noise removal algorithm with an impulse detector. IEEE Trans. Image Process. **14**, 1747–1754 (2005)
18. Chang, J.Y., Chen, J.L.: Classifier-augmented median filters for image restoration. IEEE Trans. Instrum. Meas. **53**, 351–356 (2004)
19. Yuan, S.Q., Tan, Y.: H.: Impulse noise removal by a global-local noise detector and adaptive median filter. Signal Process. **86**, 2123–2128 (2006)
20. Yamashita, N., Ogura, M., Lu, J.: A random-valued impulse noise detector using level detection. In: Proceedings of the IEEE International Symposium on Circuits and Systems (ISCAS'2005), vol. 6, pp. 6292–6295. Kobe (2005)
21. Smolka, B., Chydzinski, A.: Fast detection and impulsive noise removal in color images. Real-Time Imaging **11**, 389–402 (2005)
22. Eng, H.L., Ma, K.K.: Noise adaptive soft-switching median filter. IEEE Trans. Image Process. **10**, 242–251 (2001)
23. Yüksel, M.E., Beşdok, E.A.: simple neuro-fuzzy impulse detector for efficient blur reduction of impulse noise removal operators for digital images. IEEE Trans. Fuzzy Syst. **12**, 854–865 (2004)
24. Schulte, S., Nachtegael, M., De Witte, V., Van der Weken, D., Kerre, E.E.: A fuzzy impulse noise detection and reduction method. IEEE Trans. Image Process. **15**, 1153–1162 (2006)
25. Abreu, E., Mitra, S. K.: A signal-dependent rank-ordered mean (SD-ROM) filter—a new approach for removal of impulses from highly corrupted images. In: Proceedings of the IEEE International Conference on Acoustics, Speech and, Signal Processing (ICASSP'95), vol. 4, pp. 2371–2374 (1995)
26. Abreu, E., Lightstone, M., Mitra, S.K.: A new efficient approach for the removal of impulse noise from highly corrupted images. IEEE Trans. Image Process. **5**, 1012–1025 (1996)
27. Moore, M. S., Gabbouj, M., Mitra, S. K.: Vector SD-ROM filter for removal of impulse noise from color images. In: Proceedings of ECMCS99 EURASIP Conference on DSP for Multimedia Communications and Services. Krakow (1999)
28. Mitra, S.K., Sicuranza, G.L., Gibson, J.D.: Nonlinear Image Processing (Communications, Networking and Multimedia). Academic Press, Orlando (2001)
29. Abreu, E.: Signal-dependent rank-ordered mean (SD-ROM) filter. In: Mitra, S.K., Sicuranza, G.L., Gibson, J.D. (eds.) Nonlinear Image Processing (Communications, Networking and Multimedia), pp. 111–133. Academic Press, Orlando (2001)

30. Han, W.Y., Lin, J.C.: Minimum-maximum exclusive mean (MMEM) filter to remove impulse noise from highly corrupted images. Electron. Lett. **33**, 124–125 (1997)
31. Singh, K. M., Bora, P. K., Singh, B. S.: Rank ordered mean filter for removal of impulse noise from images. In: Proceedings of the IEEE International Conference on Industrial Technology (ICIT'02), vol. 2, pp. 980–985 (2002)
32. Zhang, D. S., Kouri, D. J.: Varying weight trimmed mean filter for the restoration of impulse noise corrupted images. In: Proceedings of the IEEE International Conference on Acoustics, Speech and, Signal Processing (ICASSP'05), vol. 4, pp. 137–140 (2005)
33. Luo, W.: An efficient detail-preserving approach for removing impulse noise in images. IEEE Signal Proc. Lett. **13**, 413–416 (2006)
34. Beşdok, E., Çivicioglu, P., Alçi, M.: Impulsive noise suppression from highly corrupted images by using resilient neural networks. Lecture Notes in Artificial Intelligence, vol. 3070, pp. 670–675 (2004)
35. Cai, N., Cheng, J., Yang, J.: Applying a wavelet neural network to impulse noise removal. In: Proceedings of the International Conference on Neural Networks and, Brain (ICNN&B'05), vol. 2, pp. 781–783 (2005)
36. Russo, F., Ramponi, G.: A fuzzy filter for images corrupted by impulse noise. IEEE Signal Process. Lett. **3**, 168–170 (1996)
37. Choi, Y.S., Krishnapuram, R.: A robust approach to image enhancement based on fuzzy logic. IEEE Trans. Image Process. **6**, 808–825 (1997)
38. Russo, F.: FIRE operators for image processing. Fuzzy Sets Syst. **103**, 265–275 (1999)
39. Van De Ville, D., Nachtegael, M., Van der Weken, D.: Noise reduction by fuzzy image filtering. IEEE Trans. Fuzzy Syst. **11**, 429–436 (2003)
40. Morillas, S., Gregori, V., Peris-Fajarne, G.: A fast impulsive noise color image filter using fuzzy metrics. Real-Time Imaging **11**, 417–428 (2005)
41. Russo, F.: Noise removal from image data using recursive neuro-fuzzy filters. IEEE Trans. Instrum. Meas. **49**, 307–314 (2000)
42. Yüksel, M.E., Baştürk, A.: Efficient removal of impulse noise from highly corrupted digital images by a simple neuro-fuzzy operator. Int. J. Electron. Commun. (AEÜ) **57**, 214–219 (2003)
43. Beşdok, E., Çivicioglu, P., Alçi, M.: Using an adaptive neuro-fuzzy inference system-based interpolant for impulsive noise suppression from highly distorted images. Fuzzy Sets Syst. **150**, 525–543 (2005)
44. Kong, H., Guan, L.: Detection and removal of impulse noise by a neural network guided adaptive median filter. In: Proceedings of the IEEE International Conference on Neural Networks, vol. 2, pp. 845–849 (1995)
45. Lee, C.S., Kuo, Y.H., Yu, P.T.: Weighted fuzzy mean filter for image processing. Fuzzy Sets Syst. **89**, 157–180 (1997)
46. Lee, C.S., Kuo, Y.H.: The important properties and applications of the adaptive weighted fuzzy mean filter. Int. J. Intell. Syst. **14**, 253–274 (1999)
47. Windyga, P.S.: Fast impulse noise removal. IEEE Trans. Image Process. **10**, 173–179 (2001)
48. Smolka, B., Plataniotis, K.N., Chydzinski, A.: Self-adaptive algorithm of impulsive noise reduction in color images. Pattern Recognit. **35**, 1771–1784 (2002)
49. Rahman, S.M.M., Hasan, M.K.: Wavelet-domain iterative center weighted median filter for image denoising. Signal Process. **83**, 1001–1012 (2003)
50. Russo, F.: Impulse noise cancellation in image data using a two-output nonlinear filter. Measurement **36**, 205–213 (2004)
51. Xu, H., Zhu, G., Peng, H.: Adaptive fuzzy switching filter for images corrupted by impulse noise. Pattern Recognit. Lett. **25**, 1657–1663 (2004)
52. Alajlan, N., Kamel, M., Jernigan, E.: Detail preserving impulsive noise removal. Signal Process. Image Commun. **19**, 993–1003 (2004)
53. Yüksel, M.E., Baştürk, A., Beşdok, E.: Detail preserving restoration of impulse noise corrupted images by a switching median filter guided by a simple neuro-fuzzy network. EURASIP J. Appl. Signal Process. **2004**, 2451–2461 (2004)

54. Yüksel, M.E.: A hybrid neuro-fuzzy filter for edge preserving restoration of images corrupted by impulse noise. IEEE Trans. Image Process. **15**, 928–936 (2006)
55. Karnik, N.N., Mendel, J.M.: Application of type-2 fuzzy logic system to forecasting of time-series. Inf. Sci. **120**, 89–111 (1999)
56. Liang, Q., Mendel, J.M.: Equalization of nonlinear time-varying channels using type-2 fuzzy adaptive filters. IEEE Trans. Fuzzy Syst. **8**, 551–563 (2000)
57. John, R.I., Innocent, P.R.: Barnes MR Neuro-fuzzy clustering of radiographic tibia image data using type-2 fuzzy sets. Inf. Sci. **125**, 203–220 (2000)
58. Liang, Q.: Mendel JM MPEG VBR video traffic modeling and classification using fuzzy techniques. IEEE Trans. Fuzzy Syst. **9**, 183–193 (2001)
59. Hagras, H.: A hierarchical type-2 fuzzy logic control architecture for autonomous mobile robots. IEEE Trans. Fuzzy Syst. **12**, 524–539 (2004)
60. Lynch, C., Hagras, H., Callaghan, V.: Embedded type-2 FLC for real-time speed control of marine and traction diesel engines. In: Proceedings of the FUZZ-IEEE 2005, pp. 347–352, Reno (2005)
61. Astudillo, L., Castillo, O., Melin, P.: Intelligent control of an autonomous mobile robot using type-2 fuzzy logic. J. Eng. Lett. **13**, 93–97 (2006)
62. Gu, L., Zhang, Y.Q.: Web shopping expert using new interval type-2 fuzzy reasoning. Soft Comput. **11**, 741–751 (2007)
63. Dereli, T., Baykasoglu, A., Altun, K.: Industrial applications of type-2 fuzzy sets and systems: a concise review. Comput. Ind. **62**, 125–137 (2011)
64. Mendel, J. M.: Uncertain Rule-Based Fuzzy Logic Systems: Introduction and New Directions. Prentice-Hall International Inc, Upper Saddle River (2001)
65. Mendel, J.M., John, R.I.B.: Type-2 fuzzy sets made simple. IEEE Trans. Fuzzy Syst. **10**, 117–127 (2002)
66. Tizhoosh, H.R.: Image thresholding using type II fuzzy sets. Pattern Recognit. **38**, 2363–2372 (2005)
67. Mendoza, O., Melin, P., Licea, G.: A new method for edge detection in image processing using interval type-2 fuzzy logic. In: Proceedings of IEEE International Conference on Granular Computing 2007, pp. 151–156. Silicon Valley (2007)
68. Bustince, H., Barrenechea, E., Pagola, M.: Interval-valued fuzzy sets constructed from matrices: application to edge detection. Fuzzy Sets Syst. **160**, 1819–1840 (2009)
69. Melin, P.: Interval type-2 fuzzy logic applications in image processing and pattern recognition. In: Proceedings of IEEE International Conference on Granular Computing 2010, pp. 728–731. Silicon Valley (2010)
70. Melin, P., Mendoza, O., Castillo, O.: An improved method for edge detection based on interval type-2 fuzzy logic. Expert Syst. Appl. **37**, 8527–8535 (2010)
71. Bansal, R., Sehgal, P., Bedi, P.: A novel framework for enhancing images corrupted by impulse noise using type-II fuzzy sets. In: Proceedings of Fifth International Conference on Fuzzy Systems and Knowledge Discovery, pp. 266–271. Shandong (2008)
72. Sun, Z., Meng, G.: An image filter for eliminating impulse noise based on type-2 fuzzy sets. In: Proceedings of International Conference on Audio, Language and Image Processing 2008, pp. 1278–1282. Shanghai (2008)
73. Yildirim, M.T., Baştürk, A., Yüksel, M.E.: Impulse noise removal from digital images by a detail-preserving filter based on type-2 fuzzy Logic. IEEE Trans. Fuzzy Syst. **16**, 920–928 (2008)
74. Murugeswari, P., Manimegalai, D.: Noise reduction in color image using interval type-2 fuzzy filter (IT2FF). Int. J. Eng. Sci. Technol. **3**, 1334–1338 (2011)
75. Madasu, H., Verma, O.P., Gangwar, P.: Fuzzy edge and corner detector for color images. In: Proceedings of Sixth International Conference on Information Technology: New Generations, pp. 1301–1306. Las Vegas (2009)
76. Jeon, G., Anisetti, M., Bellandi, V.: Designing of a type-2 fuzzy logic filter for improving edge-preserving restoration of interlaced-to-progressive conversion. Inf. Sci. **179**, 2194–2207 (2009)